THE JOURNAL OF BIOLOGICAL CHEMISTRY
Vol. 272, No. 36, Issue of September 5, pp. 22630–22641, 1997

Printed in U.S.A.

The Receptor Binding Site of Human Interleukin-3 Defined by Mutagenesis and Molecular Modeling*

(Received for publication, April 10, 1997, and in revised form, June 13, 1997)

Barbara K. Klein‡§, Yiqing Feng‡§, Charles A. McWherter, William F. Hood, Kumnan Paik, and John P. McKearn

From G. D. Searle and Company, St. Louis, Missouri 63198

Interleukin-3 (IL-3) is a member of the cytokine superfamily that promotes multi-potential hematopoietic cell growth by interacting with a cell surface receptor composed of α and β chains. The newly available three-dimensional structure of a variant of human (h) IL-3 allowed us to evaluate new and existing mutagenesis data and to rationally interpret the structure-function relationship of hIL-3 on a structural basis. The amino acid residues that were identified to be important for hIL-3 activity are grouped into two classes. The first class consists of largely hydrophobic residues required for the structural integrity of the protein, including the residues in IL-3 that are largely conserved among 10 mammalian species. These residues form the core of a scaffold for the second class of more rapidly diverging solvent-exposed residues, likely to be required for interaction with the receptor. Ten important and solvent-exposed residues, Asp^{21}, Gly^{42}, Glu^{43}, Gln^{45}, Asp^{46}, Met^{49}, Arg^{94}, Pro^{96}, Phe^{113}, and Lys^{116}, map to one side of the protein and form a putative binding site for the α subunit of the receptor. A model of the IL-3·IL-3 receptor complex based on the human growth hormone (hGH)·hGH soluble receptor complex structure suggests that the interface between IL-3 and the IL-3 receptor α subunit consists of a cluster of hydrophobic residues flanked by electrostatic interactions. Although the IL-3/IL-3 receptor β subunit interface cannot be uniquely located due to the lack of sufficient experimental data, several residues of the β subunit that may interact with Glu^{22} of IL-3 are proposed. The role of these residues can be tested in future mutagenesis studies to define the interaction between IL-3 and IL-3 receptor β subunit.

Interleukin-3 (IL-3)[1] is a multi-lineage hematopoietic growth factor that promotes the growth of most lineages of blood cell precursors (1, 2). It belongs to the helical cytokine superfamily and is further classified as a short chain cytokine similar to granulocyte-macrophage colony-stimulating factor (GM-CSF) and interleukin-5 (IL-5) (3–5). Characteristic of the short chain helical cytokines, the structural core of the hIL-3 variant SC-65369 (6, 7) consists of an up-up-down-down four-helical bundle (designated as helix A through D) with a 30–40° packing angle. This helical bundle motif is completed by long overhand loops connecting the helices (loops AB and CD) and a type II turn (turn BC) between helices B and C. Distinct from the other short chain cytokines, the hIL-3 variant structure also revealed that loop AB contains an additional helix (helix A′) that is approximately parallel to helix D and interacts extensively with both helix D and loop CD. Furthermore, loop AB, which passes in front of helix D, has a threading topology that is more like that of the long chain cytokines such as growth hormone (8, 9).

Binding to a cell surface receptor (IL-3R) composed of at least α and β chains is the initial event in the expression of IL-3's proliferative activity on a target cell. The α chain of this receptor (IL-3Rα) is specific for IL-3, whereas the β chain (β_c) is shared with the related hematopoietic cytokines GM-CSF (10) and IL-5 (11). IL-3 binds to IL-3Rα with low affinity and has no detectable affinity for β_c in the absence of IL-3Rα; high affinity binding requires the presence of both chains. Following the formation of the high affinity IL-3·IL-3R complex, signal transduction is mediated by the β chain. Although the precise stoichiometry of the IL-3 receptor has not been established, we refer to the receptor as a heterodimer for simplicity.

Several approaches have been undertaken to define the regions of hIL-3 that interact with the receptor, including constructing interspecies chimeras (12, 13), mapping neutralizing and non-neutralizing anti-IL-3 monoclonal antibody epitopes (12, 14), and site-specific mutagenesis (14–20). These studies identified sequences important for activity in both N- and C-terminal regions of IL-3 and revealed many specific sites where amino acid substitutions lead to significant changes in receptor binding affinity and growth-promoting activity.

Targeted saturation mutagenesis was employed to produce over 700 single point mutants of hIL-3$_{15–125}$, which were then evaluated for expression and biological activity (19). This study identified several discrete regions of hIL-3 that are important for activity. To date, the relationships of these discontinuous regions to one another could only be inferred on the basis of secondary structure prediction and homology modeling of hIL-3 (3, 12, 17, 19). The recently available three-dimensional structure of an hIL-3 variant (7) provides for the first time an experimentally derived model to understand the effect of these mutations. In this paper, the activities of hIL-3 mutants are interpreted in terms of IL-3's three-dimensional structure. Together these data define an IL-3Rα binding site on IL-3 consisting of the solvent-exposed surface of 10 residues located on helix A, helix A′, loop CD, and helix D. These findings are exploited to construct a molecular model of the IL-3·IL-3R complex structure. This model provides explanations of the

* The costs of publication of this article were defrayed in part by the payment of page charges. This article must therefore be hereby marked "*advertisement*" in accordance with 18 U.S.C. Section 1734 solely to indicate this fact.

‡ To whom correspondence should be addressed: G. D. Searle and Co., 700 Chesterfield Pky. N., St. Louis, MO 63198. Tel.: 314-737-6240; Fax: 314-737-7223 (to B. K.); Tel.: 314-737-6046; Fax: 314-737- 7425 (to Y. F.)

§ Contributed equally to this work.

[1] The abbreviations used are: IL-3, interleukin-3; hIL-3, human interleukin-3; IL-3$_{15–125}$, a deletion variant of IL-3 consisting of residues 15–125; SC-65369, a truncation variant of IL-3 mutated in 14 of 112 positions; IL-3R, interleukin-3 receptor complex; GM-CSF, granulocyte-macrophage colony-stimulating factor; IL-5, interleukin-5; GH, growth hormone; h, human; GHR, growth hormone receptor; SA, solvent-accessible surface area; CRM, cytokine receptor motif.

mutagenesis results on the structural basis, suggests alternative ligand binding sites on IL-3Rβ, and proposes additional mutations for further investigation of the cytokine-receptor interaction.

EXPERIMENTAL PROCEDURES

IL-3 Variant Production and Characterization—Recombinant DNA procedures used to generate the IL-3 variants have been described previously (19). The plasmids were transformed into the *Escherichia coli* strain JM101 (ATCC 33876), and the variants were purified from cytoplasmic inclusion bodies (19) to greater than 90% homogeneity as determined by SDS-polyacrylamide gel electrophoresis. Circular dichroism (CD) measurements were conducted on a Jasco J500C at 20 °C. Samples for the CD experiments contained between 0.08 and 0.42 mg/ml protein in 20 mM ammonium bicarbonate at pH 4. The percentage of helical conformation was estimated from the signal at 222 nm according to Chen *et al.* (21).

Receptor Binding and Cell Proliferation Assays—Receptor binding affinity and cell proliferation activity of IL-3 variants were measured essentially as described previously (22, 23). Activity for each variant was reported as the concentration that gave 50% of the maximal response by fitting a four-parameter logistic regression model to the data. Relative potencies (EC_{50} of hIL-3 divided by EC_{50} of variant) are the mean of at least three independent assays.

hIL-3$_{15–125}$ Structure Model—A model for the wild-type hIL-3$_{15–125}$ was generated from the energy-minimized average NMR structure of the hIL-3 variant SC-65369 (Protein Data Bank entry 1JLI). The mutated residues in the structure of SC-65369 were replaced with their wild-type counterparts using INSIGHTII (Biosym Technologies, San Diego, CA). These replacements were well-tolerated because nearly all of them occur on the surface of the molecule. The resultant structure was exported into XPLOR 3.1 (24, 25), and 1000 energy minimization steps were performed while fixing the backbone N, C_α, C′, and O atoms. During the energy minimization, the electrostatic energy was included in the total energy, but the charges at the side chains of the ionizable residues, as well as at the termini, were excluded. Solvent-accessible surface area was calculated for each residue using the method of Lee and Richards (26) as implemented in XPLOR using a solvent probe radius of 1.4 Å.

hIL-3 Receptor Structural Model—Sequence alignment of the cytokine receptor motif (CRM) domains of the receptors was performed initially using the BESTFIT routine in the UWGCG Software Package (50) and subsequently manually refined using the same package. Consideration was given to previously identified consensus sequence motifs (3), secondary structure predictions, the locations of β strands and loops of growth hormone receptor (GHR) in the GH·GHR complex structure (Protein Data Bank entry 3HHR) (9), and the locations of residues that contribute to the hydrophobic cores of the GHR domains. Specific reference points employed included the locations of conserved disulfide bridges in the N-terminal domain of GHR and the "WS*X*WS box" in the C-terminal domain. The initial coordinates of the CRM domains of IL-3Rα (residues 106–294) and β_c (residues 244–439) were constructed by substituting the IL-3R sequences into the corresponding GHR structures in INSIGHTII. Extended loops were modeled from fragments of highly refined protein crystal structures in the Protein Data Bank and spliced into the receptor structures. The initial models for each subunit were exported into SYBYL (Tripos Associates, St. Louis, MO) where the side chain torsion angles were iteratively scanned for combinations that would relieve van der Waals violations. The structures were then exported to CHAIN (Baylor College of Medicine, Houston, TX) to improve the main chain geometry of the spliced loops. The resulting structures were further refined by energy minimization using XPLOR (24, 25). Initial energy minimizations were performed with all non-hydrogen atoms fixed and then repeated with all backbone atoms fixed. Subsequent full atom energy minimization employed distance and backbone dihedral angle constraints for β sheets to preserve secondary structure while still permitting side chain and segmental movements. The side chains were subject to 10 ps of molecular dynamics at 100 K and subsequently to energy minimizations with full electrostatic potentials for all atoms except for side chain atoms of ionizable residues and the termini.

IL-3·IL-3R Complex—The model for the structure of the complex was generated through several stages. Initially, key mutagenesis data were used to identify putative complementary residues as tether points to place IL-3 in the ligand binding pocket. IL-3 and the receptor were then subject to rigid body movement tethered with distances from the side chain carboxyl group of IL-3 Asp^{21} to the center of the charged side chain atoms of IL-3Rα Arg^{234}, Lys^{235}, and Arg^{277}, and from the carboxyl group of IL-3 Glu^{43} to the center of the charged side chain atoms of IL-3Rα Arg^{145} and Arg^{146} constrained to be ≤5.0 Å. There is sufficient space between the two subunits in the receptor model so that no movement of the β_c subunit was required when IL-3 is docked to the α subunit. Next, a full atom energy minimization of the complex (except for backbone atoms of IL-3Rα residues 211–294 and β_c residues 343–439, sequences that are involved primarily in the intersubunit interface) was carried out using the same ligand-receptor distance constraints as described above. This minimization excluded electrostatic interactions, and it used distance and backbone dihedral angle constraints to maintain secondary structures in both IL-3 and its receptor. A subsequent round of energy minimization included electrostatic contributions for all atoms except for charged atoms of ionizable side chains and termini. At the final stage, the minimization was carried out with full electrostatic potentials for all atoms except for chain termini. The solvent-accessible areas buried upon complex formation were calculated in XPLOR using a probe size of 1.4 Å.

Electrostatic Potential Calculations—The electrostatic potentials surrounding hIL-3$_{15–125}$ and the receptor were calculated using GRASP (27). The Amber parameter set was used to assign partial charges. Dielectric constants of 80 and 2 were assigned to the solvent and the solute, respectively. The ionic strength of the solvent was set to 145 mM, the water probe radius to 1.4 Å, and the ionic radius to 2 Å. A charge of 0.5 unit was assigned to histidine side chains. Because only the CRM domains of the receptor sequences were used in modeling, the beginning and end of the receptor chains were left uncharged.

RESULTS AND DISCUSSION

An extensive screening mutagenesis study was carried out using hIL-3$_{15–125}$ as the template (19) to identify amino acid residues important for biological activity. Libraries of single point mutants were created at nearly 90% of the positions using polymerase chain reaction mutagenesis methods. The resulting mutants were expressed for secretion in *E. coli*, and the secreted proteins were recovered after osmotic shock. Their bioactivity was measured using an IL-3-dependent cell proliferation assay, and protein concentrations were determined by enzyme-linked immunosorbent assay. The activities were evaluated for mutations at 97 of the 111 sites (with an average of eight amino acid substitutions at each position) to evaluate their tolerance to substitution. The results indicated that for >70% of the residues evaluated, substitution by other amino acids with a variety of size, polarity, and charge maintained significant level of biological activity. For the purpose of the following discussion, a residue is considered to be intolerant to substitution when, of at least three substitutions tested, no more than one had greater than 5% of the proliferation activity of the parental molecule. Residues that were found to have approximately half active (≥5% of hIL-3 activity) and half inactive (<5% of hIL-3 activity) substitutions are classified as partially tolerant. Residues where the majority of the mutations have >5% activity are considered tolerant. Using these criteria, the results reported previously by Olins *et al.* (19) are summarized in Table I. A total of 16 amino acid residues are classified as intolerant, and another 12 are classified as partially tolerant. Substitution-sensitive residues, consisting of both intolerant and partially tolerant residues, are distributed throughout the linear sequence of the protein.

A model for hIL-3$_{15–125}$ was derived from the recently determined NMR structure of the hIL-3 variant SC-65369 (7). In addition to N- and C-terminal truncations of 13 and 8 residues, respectively, SC-65369 contains 14 amino acid substitutions (V14A, N18I, T25H, Q29R, L32N, F37P, G42S, Q45M, N51R, R55T, E59L, N62V, S67H, and Q69E) that were found to be localized at the solvent-exposed surface of the protein. Despite the number of amino acid substitutions, both biophysical and biochemical data (7) indicate that the structural features of SC-65369 are relevant for wild-type hIL-3. In comparison to native IL-3, SC-65369 is fully active in both cell proliferation

TABLE I
Amino acid residues sensitive to substitution (see text) and conserved in mammalian IL-3 sequences

Position	Class[a]	SA area[b]	Conservation[c]
Cys^{16}	I	20.6	ex, ov, bo
Ile^{20}	PT	0.0	ch, gi, rh
Asp^{21}	PT	68.4	ch, gi, rh
Glu^{22}	I	81.9	all
Ile^{23}	T	0.7	all
Ile^{24}	PT	26.2	ch, gi, rh, mu
Leu^{27}	I	2.2	all
Glu^{43}	I	128.4	primate
Asp^{44}	I	22.7	primate
Ile^{47}	PT	7.2	primate, ov
Leu^{48}	I	0.0	all
Met^{49}	PT	111.6	ch, gi, ta, ma
Asn^{52}	PT	8.5	primate
Leu^{53}	I	0.6	ex, mu
Arg^{54}	PT	1.2	primate, mu
Asn^{57}	ND	0.0	all
Leu^{58}	I	0.0	all
Phe^{61}	I	0.0	all
Ala^{64}	I	12.1	ex, ra, mu
Leu^{68}	PT	3.3	primate
Ile^{74}	ND	10.4	all
Leu^{78}	ND	0.3	all
Leu^{81}	I	0.0	ex, ov, bo
Cys^{84}	I	45.4	ex, ov, bo
Pro^{86}	T	45.4	all
Arg^{94}	I	100.3	ch, gi, rh
Pro^{96}	I	54.0	primate
Ile^{97}	PT	8.9	ex, mu
Ile^{99}	PT	7.9	all
Gly^{102}	PT	10.1	primate
Phe^{107}	ND	1.3	all
Lys^{110}	I	2.5	all
Leu^{111}	ND	0.3	all
Phe^{113}	ND	49.6	ex, ov, bo
Leu^{115}	I	0.0	ex, mu, ra
Thr^{117}	PT	16.7	ex, bo

[a] Sensitivity to amino acid substitution: I, intolerant; PT, partially tolerant; T, tolerant; ND, not determined.
[b] Indicates the solvent-accessible area (in Å^2) for the given residue in the three-dimensional model of hIL-$3_{15–125}$.
[c] Extent of conservation at a given position: ch, chimpanzee; gi, gibbon; rh, rhesus; ov, ovine; bo, bovine; ra, rat; mu, mouse; ex, except.

and cell surface IL-3Rα binding assays, and it has a similar helical content as determined by CD spectroscopy.[2]

Distinguishing Structurally Important Residues from Receptor Contact Residues—Residues that are sensitive to substitution may be so either because they are important for receptor contact and their substitution diminishes the complementarity required for optimal receptor recognition, or because they are important for structural integrity and their substitution deranges the structure, thereby indirectly distorting the recognition site. Correlating solvent accessibility with sensitivity to substitution is one approach to assess the role of an amino acid residue in protein-protein interaction.

Solvent-accessible surface areas (SA) for individual residues in hIL-$3_{15–125}$ are presented in Fig. 1. Fifteen out of the total of 28 substitution-sensitive residues in Table I are found to be hydrophobic (Ala, Phe, Ile, Leu, Val, Met, Trp). Met^{49} is the only hydrophobic and substitution-sensitive residue with a large solvent exposure (SA = 112 Å^2). The remainder are largely buried inside the structure (SA $\leq$30 Å^2). Among the non-hydrophobic residues classified as intolerant to substitution, Cys^{16} and Cys^{84} form the only disulfide bridge in hIL-3. Studies on both hIL-3 variants[3] and mouse IL-3 (28) indicated that this disulfide bond is required for bioactivity and may do so by stabilizing the tertiary structure. In addition to the above residues, five of the substitution-sensitive yet hydrophilic residues (Asp^{44}, Asn^{52}, Arg^{54}, Lys^{110}, and Thr^{117}) are also buried in the structure (Fig. 1 and Table I). These residues are likely to stabilize the structure through internal salt bridging and/or hydrogen bonding interactions (see below).

While greater than two-thirds of the substitution-sensitive residues are involved in maintaining the three-dimensional structure of hIL-3, six (Asp^{21}, Glu^{22}, Glu^{43}, Met^{49}, Arg^{94}, and Pro^{96}) have significant solvent-accessible area (>50 Å^2) and are good candidates for being involved in direct contacts with the receptor.

Cell Proliferation Activity and Receptor Binding Affinity of Purified Variants—To confirm the results of the screening mutagenesis studies and to test the effect of the mutations on receptor binding properties, several point mutants were selected for purification and full characterization. Mutants were chosen on the basis of their sensitivity to substitution, solvent accessibility, and location in the three-dimensional structure (Table II). The genes encoding the point mutants were transferred to an *E. coli* cytoplasmic expression system, expressed, and purified to homogeneity. To rule out the possibility that structural perturbation leads to the loss of activity, seven of the mutants (G42A, G42D, E43N, D44A, E50D, F113Y, and K116W), along with the parental molecule hIL-$3_{15–125}$, were characterized using far UV circular dichroism spectroscopy. All of the variants had a helical content of ~40% that was indistinguishable from that of hIL-$3_{15–125}$ and was also consistent with the solution structure of SC-65369 (6). These data indicate that the mutants are properly folded with no large scale changes in global conformation.

The cell proliferation activity and IL-3Rα binding affinity of these purified variants are listed in Table II. Significantly decreased (>5-fold) growth-promoting activity was found for E22G (helix A), E43N (helix A′), D44A (helix A′), and L115M (helix D), in agreement with the screening mutagenesis studies (19). A fifth mutant, F113Y (helix D), also showed sharply decreased growth-promoting activity. This mutant, which did not express in the screening mutagenesis study, was chosen because it is the only hydrophobic residue on helix D with significant solvent exposure (SA = 50 Å^2) and because helix D has been implicated in the receptor binding of both hIL-3 (17, 19) and GH (9).

A good correlation was observed between the cell proliferation activity of a variant and its binding affinity to IL-3Rα (Table II). For example, relative to hIL-3, variants E43N and F113Y bind to the α subunit with less than 20% of hIL-3's affinity and have a similar diminution (15–20%) in their growth-promoting activity. Similarly, variants such as G42A, Q45V, D46S, and K116W show strong increases in both IL-3Rα binding and cell proliferation activity. These findings suggest that these mutations exert an effect on the initial binding event, *i.e.* binding to the α subunit. The only significant exceptions to this trend are E22G and D44A. Glu^{22} has previously been described as a residue important for interacting with β_c subunit while having no effect on IL-3Rα binding (18, 29). The discrepancy between IL-3Rα binding affinity and cell proliferation activity of D44A may be the result of decreased stability of this mutant (see below). In contrast to residues that were found to be intolerant to substitution, most residues whose mutation resulted in increased cell proliferative activity (see Table III in Ref. 19) are readily accessible to solvent (Fig. 1).

Structurally Important and Evolutionarily Conserved Residues—The role of the important yet buried residues in helical packing is illustrated in Fig. 2. These residues are clustered at interior helical interfaces. A similar clustering pattern was observed for residues that are conserved evolutionarily. In ad-

[2] R. Schilling, unpublished results.
[3] R. McKinnie and B. Klein, unpublished results.

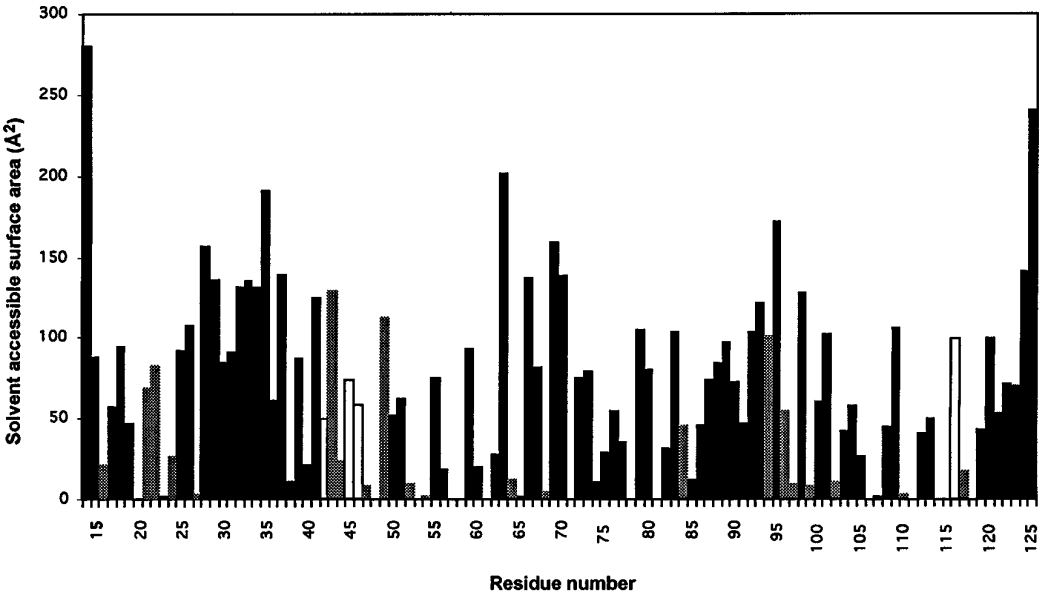

FIG. 1. **Solvent-accessible areas of hIL-$3_{15–125}$.** The solvent-accessible area for each amino acid residue in the energy-minimized model of hIL-$3_{15–125}$ was calculated using a 1.4-Å probe. The *open bars* indicate residues where variants of increased activity were identified, and the *gray bars* represent residues that were intolerant or partially tolerant to substitution (see text). Caution should be exercised for the amount of the buried surface for residues 28–39 because the flexibility this sequence exhibits in the three-dimensional structure makes its precise position uncertain.

TABLE II
Relative activities of a selected set of purified hIL-3 variants

Summary of cell proliferation activity and low affinity receptor binding activity of selected single point variants in hIL-$3_{15–125}$. Assays are described under "Experimental Procedures."

Position	Substitution	Relative binding[a]	Relative AML activity[b]
hIL-$3_{15–125}$		1.7	2.5[c]
Glu^{22}	Gly	1.3	0.008
Gly^{42}	Asp	16	9[c]
Gly^{42}	Ala	11	3.2
Glu^{43}	Asn	<0.2	0.1
Asp^{44}	Ala	1.1	0.2
Gln^{45}	Val	18	8[c]
Asp^{46}	Ser	7	10[c]
Glu^{50}	Asp	7	7[c]
Phe^{113}	Tyr	<0.2	0.15
Leu^{115}	Met	<0.2	0.04
Lys^{116}	Val	2	8[c]
Lys^{116}	Trp	50	26[c]
Gln^{122}	Phe	1.4	6[c]

[a] Low affinity binding (α receptor subunit only) measured relative to hIL-$3_{1–133}$.
[b] Cell proliferation activity expressed relative to hIL-$3_{1–133}$.
[c] Data from Olins *et al.* (19).

dition to human IL-3, sequences for nine other mammalian IL-3s are available as follows: chimpanzee, rhesus, gibbon, tamarin, marmoset, sheep, bovine, mouse, and rat (30, 31).[4] The alignment of all 10 IL-3 sequences is shown in Fig. 3 with the five helical segments identified in the SC-65369 structure indicated.

Significant amino acid divergence is observed even for the six primate sequences. This is consistent with the limited cross-species functionality of primate IL-3s. For example, IL-3 from the new world monkeys (tamarin and marmoset) are not active against human cell lines (*e.g.* AML-193 cells (30)). There are 14 residues that are identical through all 10 species (Fig. 3) as follows: Glu^{22}, Ile^{23}, Leu^{27}, Leu^{48}, Asn^{57}, Leu^{58}, Phe^{61}, Ile^{74}, Leu^{78}, Pro^{86}, Phe^{107}, Lys^{110}, Leu^{111}, and Tyr^{114}. According to the structure of SC-65369, 10 of the 14 strictly conserved residues are buried hydrophobic residues with solvent-accessible areas of less than 15 $Å^2$ (Fig. 1 and Table I). Two other identical residues, the positively charged Lys^{110} and the polar Asn^{57}, are also buried in the structure. The remaining two strictly conserved residues, Glu^{22} and Pro^{86}, are largely exposed to solvent.

There is an extensive overlap in the lists of residues identified to be important by mutagenesis and those that are conserved across species. Only one of the conserved residues, Ile^{23}, was found to be tolerant of substitution in hIL-$3_{15–125}$. Even in this case, amino acid replacements that resulted in active variants were limited to hydrophobic residues. Similarly, for most of the substitution-sensitive residues identified in hIL-$3_{15–125}$, only conservative amino acid substitutions were found in the other mammalian IL-3 sequences. One exception is the substitution I20R, which occurs in both the tamarin and marmoset sequences. The structure suggests that this substitution would place a charged residue in the hydrophobic core, and this would therefore severely disturb the packing of helix A in the absence of any compensatory substitution(s). Indeed this change by itself is not tolerated in hIL-$3_{15–125}$. The potential packing defect this substitution would create in tamarin and marmoset IL-3 may be offset by concerted substitutions occurring nearby, such as M19L and N120I.

Approximately half of the hIL-$3_{15–125}$ variants with substitutions at conserved residues failed to express at levels greater than 1 μg/ml in the *E. coli* secretion system (Fig. 2), suggesting that substitutions at these positions resulted in proteins that could not adopt a stably folded conformation. The low protein expression levels prevented the evaluation of the activity of most of these variants.

Several charged and/or hydrophilic residues are also suggested to participate in the core structure of hIL-3 (7). Residues Asp^{44}, Asn^{52}, Arg^{54}, Asn^{57}, Lys^{110}, and Thr^{117} all have small solvent-accessible areas (Table I) and are sensitive to substitution. This sensitivity can be understood by describing their roles in maintaining structural integrity. The basic residue Lys^{110} in helix D, which is conserved among the 10 mammalian species and is sensitive to substitution in hIL-$3_{15–125}$, is implicated in an internal salt bridge to stabilize the protein structure. Two acidic residues, Asp^{44} in helix A′ and Glu^{106} in helix

[4] S. M. Mwangi, L. L. Logan-Henfrey, and B. Mertens, unpublished information.

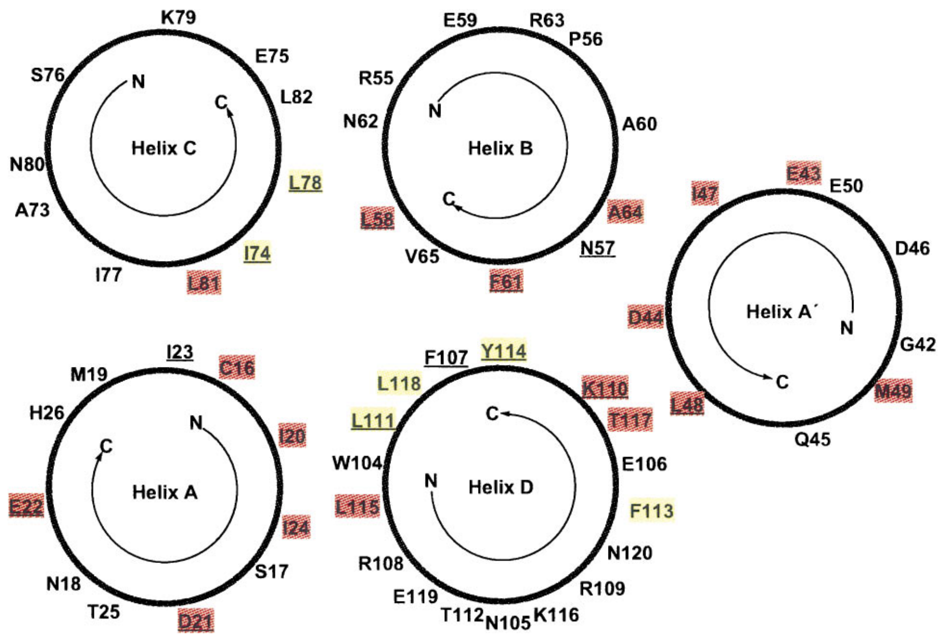

FIG. 2. **Schematic of the hIL-3 structural core.** Helix A and helix B are viewed from their N termini, and helix A′, helix C, and helix D are viewed from their C termini. Residues that are sensitive to amino acid substitution as determined by saturation mutagenesis are indicated in *red*. Mutations where low protein expression level (less than 1 μg/ml) limited evaluation by saturation mutagenesis are indicated in *yellow*. Amino acid residues that are conserved in the 10 known mammalian IL-3 sequences are *underlined*. Residues 16, 57, and 107 in this figure were not evaluated in the screening mutagenesis.

```
                     10        20        30        40        50        60        70
human       APMTQTTPLKTSWV-NCSNMIDEIITHLKQPPLPLLDFNNLNGEDQDILMENNLRRPNLEAFNR-AVK-SLQN
chimapanzee .......S......-..................................................-...-....
gibbon      .......S......-.................................................K-...-....
rhesus      .......S.....A-K............N.....SP......E...T..V.K....S.....SK-...-....
tamarin     .AP....S..ATQ.-....LRE..V.L.N......SSN....R...R...KP..........QK-...-....
marmoset    .AP...M....TQ.-....LRE..V.L.N.....ASSN....R...R...KP...K......QK-...-....
sheep       ..QA.GL..R.PRT-PY.SLME..MDD..--IT.SPEGS...SDEKN..ANKS.LQA..K..MTF.TD-TFGS
bovine      ..QAKGL.VV..RT-PY.MLMK..MDD..--IT.SPEGS...SDEKNF.TKES.LQA..KV.MTF.TD-TFGS
mouse       .SISGRDTHRLTRTL...SIVK...GK.PE.E.K-------TDDEGPS.RNKSF..V..SK.VESQGEVDPED
rat         ISDRGSDAHHLLRTLD.RTIAL..LVK.PVSG.N-------.SD.KAN.RNST...V..DE.LKSQEEFDS.D
conserved                         EI   L               aa   L    h   NL  F
helical regions

                   80        90        100       110       120       130
human       ASAIESILKNLLPCLPLATAAPTRHPIHIKDGDWNEFRRKLTFYLKTLENAQAQQTTLSLAIF
chimapanzee ...........................R..................................F
gibbon      ...........P....M..........R.............K........E....M....E.S
rhesus      ...........P....M.......P..R.TN..R.D.....K........E...
tamarin     .T....S..D.PL...M..N.SMQ...R.......D..M..K.......IK.P.
marmoset    .A....N..D.PV...T..N...Q...R.......D.QM..K.......IK.P.
sheep       ..K.MKN..EFQ.V..T..--..EDS.L.E.SNLGD..M..EE..A.IRGYLRHDLAAAET.
bovine      D.K.MKN..EFQ.V..T..--..ED..F.ENKNLGD..M..EE..VIIR.YLK-----.KN.WFS
mouse       RYV.K.N.QK.NC.I.TSANDSALPGVF.R--.LDD..K..R..MVH.NDLETVL.SRPPQPASGSV SPNRGTVEC
rat         TTD.K.K.QK.KC.I.A.ASDSVLPGVYN.--.LDD.KK..R..VIH.KDL.PVSVSRPPQPTSSSD NFRPMTVEC
conserved      I   L  h   hP                   aF  KL  Y   h
helical regions
```

FIG. 3. **Sequence alignment of mammalian IL-3.** Alignment of amino acid sequences from 10 mammalian species. *Dashes* represent gaps in the alignment. Amino acid residues conserved in all 10 species are indicated under *conserved*. Functionally conserved residues are also indicated under *conserved* by *a* (acidic) or *h* (hydrophobic). Helical regions determined in the SC-65369 structure are indicated by *horizontal bars*. The alignment was obtained from the pile-up algorithm in the Genetics Computer Group (Madison, WI).

D (both functionally conserved across mammalian IL-3 sequences), reside in close proximity to Lys^{110} (see Fig. 4). Asp^{44} may be more critical for a charge-pair interaction with Lys^{110} because position 44 can only tolerate the conservative substitution of glutamic acid, whereas Glu^{106} is tolerant to a wide variety of amino acid substitutions (19). Although the variant D44A maintains native-like receptor binding affinity, it is significantly less stable to urea denaturation than hIL-3_{15-125}.[5] The difference between receptor binding affinity and proliferation activity may thus reflect the stability of the molecule under the different temperatures and time scales employed in these assays. It is interesting to note that similar results were reported for IL-3 variant K110E (20), where the variant was less stable but retained significant levels of receptor binding affinity (40%) and proliferation activity (14%). As discussed in Feng *et al.* (7), Asn^{52} is poised to hydrogen bond with the backbone atoms of Thr^{89} or Ala^{91}, thereby tethering a turn in loop CD to the helical bundle. Being in a reverse turn between helix A′ and helix B, Arg^{54} can form hydrogen bond(s) to the backbone carbonyl of either Met^{49} or Leu^{48} in helix A′ to stabilize the relative orientation of these two helices. Asn^{57}, conserved and completely buried in the hIL-3_{15-125} structure, is positioned to form a hydrogen bond to the backbone of Ile^{47} in helix A′ and thus contributes to the packing of helices A′ and B.

In addition to the hydrophobic core of the four-helical bundle, the structure reveals that two moderately intolerant hydrophobic residues (Ile^{97} and Ile^{99}) that occur in loop CD are intimately packed against helices A′, B, and D, and they further

[5] B. Klein, unpublished results.

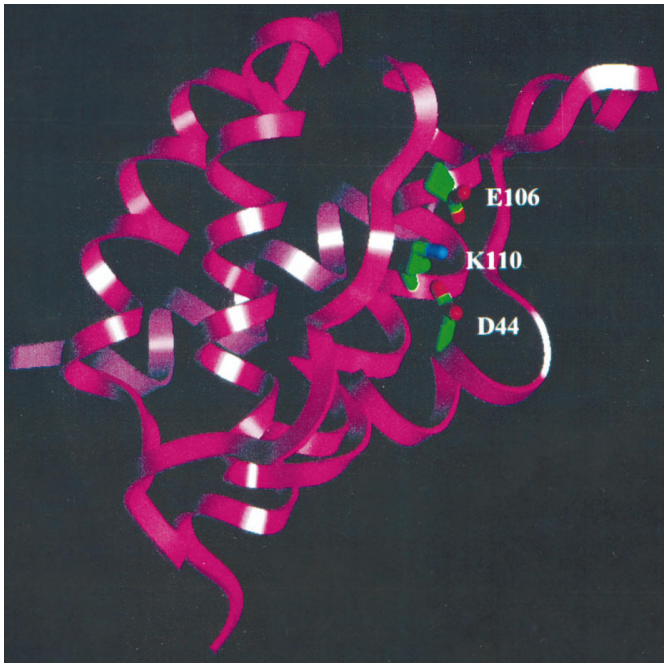

FIG. 4. **Charged residues buried in the structure.** Ribbon diagram of the three-dimensional model of hIL-3_{15-125} illustrating the buried charged residues Asp^{44}, Glu^{106}, and Lys^{110}, which are implicated in charge interactions to stabilize the core structure of the protein.

serve to maintain a structural core. Of the five charged residues found to be critical for activity, Asp^{44} and Lys^{110} are suggested to be important for stability based on analysis of the structure. In the absence of structural information, and because of their charged nature, they might have been presumed to be in direct contact with the receptor.

In summary, these results demonstrate that most of the residues found to be critical to the activity of hIL-3 reside in the interior of the protein and are therefore unlikely to directly interact with the receptor; they ensure a stable structural scaffold instead. The sensitivity that these residues exhibit to substitution must be an indirect consequence of structural perturbations that result from the unfavorable process of attempting to bury polar and charged side chains in the hydrophobic core, or by the creation of packing defects when small side chains attempt to replace bulky ones.

Putative Receptor Binding Site—The important and solvent-accessible residues identified in previous sections, Asp^{21}, Glu^{22}, Glu^{43}, Met^{49}, Arg^{94}, Pro^{96}, and Phe^{113}, are the most likely candidates to be involved in receptor binding interactions. While distant from one another along the linear sequence, these residues are in close spatial proximity in the three-dimensional structure. Solvent-accessible surface contours of the above seven residues are shown in the structure depicted in Fig. 5. When the surface contours of residues where substitutions resulted in significantly increased (≥10-fold) cell proliferation activity and/or IL-3Rα binding affinity (Gly^{42}, Gln^{45}, Asp^{46}, and Lys^{116}) are included, the surface of these 11 residues forms a continuous patch on one side of the IL-3 structure (874 $Å^2$). Mutations at seven of these residues (Asp^{21}, Gly^{42}, Glu^{43}, Asn^{45}, Asp^{46}, Phe^{113}, and Lys^{116}) have been shown in this and other work (17, 18, 20) to directly affect the binding of the ligand to IL-3Rα, whereas mutations at Glu^{22} specifically affect the binding to the β subunit (18). Therefore, we propose that the contiguous surface shown in Fig. 5 minus the surface contributed by Glu^{22} constitutes the binding site of hIL-3 for the α chain of its receptor. This site has a surface area of 792 $Å^2$ and encompasses regions in helix A (Asp^{21}), helix A′ (Gly^{42}, Glu^{43}, Gln^{45}, Asp^{46}, and Met^{49}), loop CD (Arg^{94} and Pro^{96}), and helix D (Phe^{113} and Lys^{116}).

Thus far, only Glu^{22} has been shown to affect the binding of hIL-3 to IL-3R with little, if any, change observed in binding to IL-3Rα. Thus, consistent with the results of other workers (18), we would characterize residue 22 as interacting exclusively with the β subunit. No additional β subunit contacts were identified in this work; the remaining solvent-exposed residues on helix A, *i.e.* Ser^{17}, Asn^{18}, Met^{19}, Thr^{25}, and His^{26}, were found to be tolerant to substitution. Similarly, all of the solvent-exposed residues on the neighboring helix C, *i.e.* Ala^{73}, Ser^{76}, Ile^{77}, Lys^{79}, and Asn^{80}, are tolerant to a wide variety of amino acid substitutions (19).

Comparison with Previous Mutagenesis Results—Previous structure-activity studies of hIL-3 (12–18, 20) have revealed a list of residues that are important for activity. Comparison of these results has been difficult because different methods and criteria were used to evaluate the effect of mutations, leading to different, sometimes conflicting results. For this reason, we chose to highlight several studies below.

Hybrids of mouse and gibbon IL-3 allowed Kaushansky *et al.* (12) to identify three regions (residues 15–22, 21–45, and 107–119) as essential for biological activity. Based on the fact that chimpanzee IL-3 cross-reacts with the human cell line while tamarin IL-3 does not, Dorssers *et al.* (13) used chimpanzee/tamarin interspecies chimeras to demonstrate that residues in the first two exons (residues 15–35 and 36–49, respectively) are critical for stimulating the proliferation of an hIL-3-dependent cell line. Among the site-specific mutagenesis results, hIL-3 single point mutants of residues 21 and 108 (17, 18) and double mutants of residues 101/116 and 104/105 (17) were shown to affect IL-3Rα binding and/or result in changes in biological activity. Recently, Bagley *et al.* (20) proposed an eight-residue receptor α subunit binding epitope consisting of Ser^{17}, Asn^{18}, Asp^{21}, Thr^{25}, Arg^{108}, Phe^{113}, Lys^{116}, and Glu^{119} that encompass portions of helices A and D. Other residues such as 33 and 34 (15) have also been described as being important for activity.

The work described in this paper is consistent with many aspects of previous reports regarding residues functionally important for IL-3 activity. Guided for the first time by the availability of an experimentally determined structure, we now have a structural basis to rationally interpret these results. In addition to the important amino acid residues previously identified to contact the receptor (residues 21, 22, 113, and 116), residues Gly^{42}, Glu^{43}, Gln^{45}, and Asp^{46} were shown to play a significant role in binding to the receptor α subunit, and the α subunit binding site is proposed to extend to Met^{49}, Arg^{94}, and Pro^{96}. The finding from saturation mutagenesis that no solvent-accessible critical residues reside on helix C confirms the conclusion of Bagley *et al.* (20) that was based on a limited set of mutations on helix C. The diminished activity in the chimpanzee/tamarin chimera in which the first exon was swapped can be explained by a structural perturbation in helix A upon mutation I20R.

Several residues considered to be important previously, such as residues 17, 18, 25, 101, 104, 105, 108, and 119, are not classified as critical contributors to the receptor binding interaction in this work. This difference may be attributed to the limited range of amino acid substitutions tested at these sites in the earlier studies. In particular, the detrimental effects of the substitutions S17K, N18K, T25R, R108E, and E119R (20) could be the result of introducing charged residues that altered the electrostatic potential surrounding the ligand and interfered with the proper docking of the ligand to the receptor (see below). Electrostatic potential calculations incorporating these

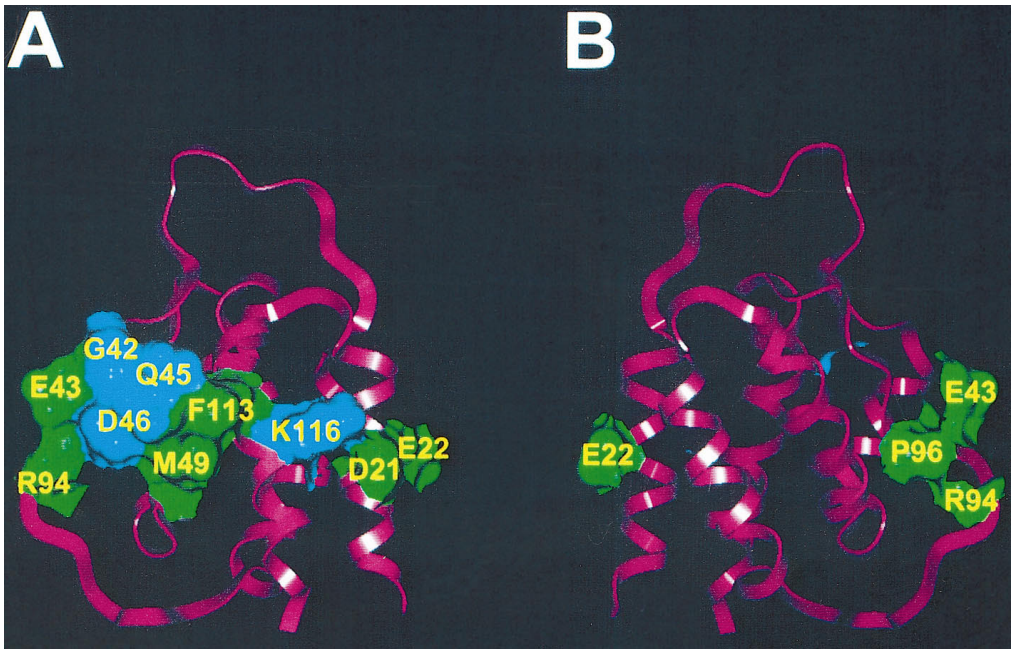

FIG. 5. **Putative hIL-3 receptor binding site.** Ribbon diagram of the three-dimensional model of hIL-$3_{15–125}$ illustrating the putative hIL-3 receptor binding site. *Green* surface contours indicate residues where amino acid substitutions significantly impair cell proliferation activity and/or receptor binding affinity. *Blue* surface contours are for residues that gave greater than 10-fold increase in cell proliferation activity and/or receptor binding affinity upon substitution. *A*, view of the structure with helices A and D in front; *B*, the molecule in *A* rotated 180° so that helices B and C are in front.

mutations indicate that such interferences are possible. The mutagenesis data thus only suggest that these residues are in the neighborhood of the receptor binding site but do not prove their direct involvement in specific interactions with the receptor due to the long range nature of the electrostatic interaction. Several neutral substitutions at these sites were found to have activity similar to native hIL-3 in the screening mutagenesis studies (19). Further studies on variants with neutral substitutions such as Ala will allow the role of these residues to be more accurately assessed. Likewise, the activity of the chimpanzee/tamarin chimera with substitutions in the second exon may have suffered from the simultaneous introduction of two positive charges (G42R and D46R) in an environment that has negative electrostatic potential appropriate for ligand docking in native hIL-3 (see below).

Comparison with Other Short Chain Cytokines—IL-3 is most closely related to two other hematopoietic cytokines, GM-CSF and IL-5, both in terms of structure and biological function. All three proteins are members of the short chain helical cytokine family (33) based on the length of the helices. The solution structure of the hIL-3 variant SC-65369 (7) has shown that the helical bundle is very similar to that of GM-CSF although significant differences exist in the loop regions. Alignment of amino acid sequences of the helical regions (7) for these related proteins showed that only six residues are identical and that five of the six (Leu^{27}, Leu^{78}, Phe^{107}, Leu^{111}, and Leu^{115}) in the hIL-3 sequence are buried hydrophobic core residues that are also conserved among mammalian IL-3 sequences. The sixth identical residue is Glu^{22} in the hIL-3 sequence that corresponds to Glu^{21} in GM-CSF and Glu^{12} in IL-5. In each case, this residue has been shown by site-directed mutagenesis to be critical for binding to β_c (18, 29, 34, 35). The limited amino acid conservation among the three proteins is not unexpected based on the lack of functional cross-reactivity among these cytokines.

Although a detailed map of the binding site of GM-CSF to the receptor has not yet been elucidated, regions in helices A (36), C (37, 38), and D (36, 39, 40), loop AB including the short β strand (39), and the extreme C terminus (37, 40) have been shown to be critical for biological activity. Of the seven solvent-exposed residues in helix A, only Glu^{21} was found to play a critical role in binding to the GM-CSF receptor (35, 36). Mutagenesis results for solvent-exposed residues in helix D of GM-CSF (36) demonstrated that only Glu^{108} and Asp^{112} showed significant sensitivity to substitution. Asp^{112} of GM-CSF corresponds to Phe^{113} in hIL-3, shown in this study to play a role in the receptor binding. The involvement of loop AB of GM-CSF including a β strand resembles the situation in IL-3, where helix A′, as a different type of secondary structure element in loop AB, is implicated in receptor binding. Therefore the sites of interaction between the cytokines and their cognate α subunits are remarkably similar. The role of residues on helix C differs between IL-3 and GM-CSF. Two studies (37, 38) revealed the importance of this region in GM-CSF, whereas no important residues were identified on the surface of helix C in hIL-$3_{15–125}$ (19, 20). This difference supports the previous conclusion that the binding of GM-CSF to β_c may be distinctly different from that of IL-3 (29).

In addition to demonstrating that Glu^{12} of IL-5 is critical for the binding of β_c, the charged amino acid residues in IL-5 were replaced either individually or in small clusters with alanine (34). The results showed that most of the charged residues were tolerant to substitution without a large decrease in cell proliferation activity. The receptor binding data together with the cell proliferation results suggested that two residues, Arg^{90} and Glu^{109}, were important for binding to the α subunit of the receptor. These residues are located in helix D, adjacent to the α subunit binding site identified in IL-3. These data again point to a similarity in the location of the binding sites between the two cytokines and the corresponding α subunits.

Comparison with hGH Receptor Binding Sites—The receptors for growth hormone, prolactin, IL-3, and many other interleukins and colony-stimulating factors are grouped into class I in the superfamily of cytokine receptors. These receptors are characterized by common cytokine binding domains and a lack of catalytic activity in their cytoplasmic domains (3). The

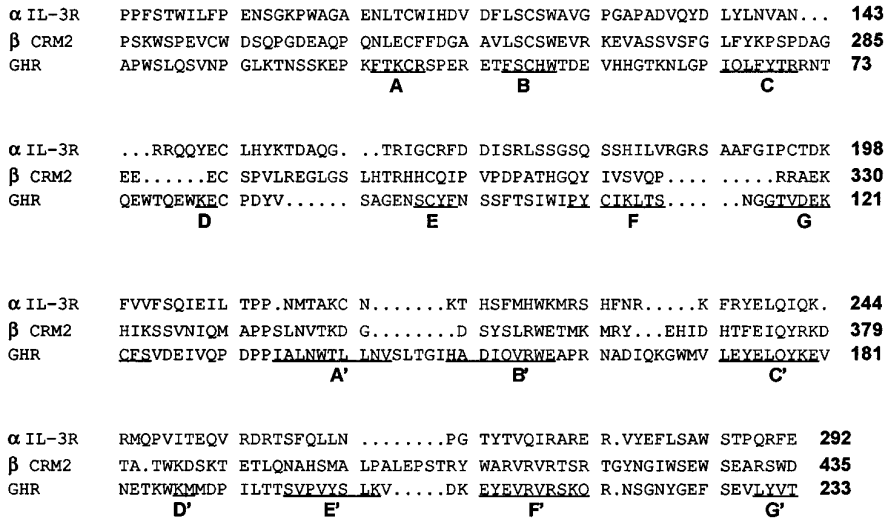

FIG. 6. **Amino acid sequence alignment of the CRM of the receptors.** The amino acid sequence alignment for the human GHR, the CRM of the α subunit of the IL-3 receptor, and the membrane proximal CRM of the β subunit of the IL-3 receptor are shown. Also indicated are the β strand regions (*underlined*) of the GH receptor as determined by the program DSSP (49).

best characterized receptor-ligand interaction among the class I receptors is the GH-soluble GHR system (9, 41, 42). Many different experimental techniques including homolog-scanning mutagenesis, alanine-scanning mutagenesis, crystallography, and plasmon resonance spectroscopy have been applied to this system, and each technique contributed uniquely to the understanding of the interaction between hGH and hGHR. Together the data define both a structural and a functional epitope (42), where the structural epitope comprises atoms that become solvent-inaccessible upon complex formation and the smaller functional epitope includes amino acid residues that contribute significantly to the binding energy of the complex.

Similarities exist between the binding sites of the GH system and the IL-3 system. Inferred from the biological activity measurement in combination with mutagenesis, the binding site proposed in this work should correspond to the functional epitope. The binding site for IL-3Rα has been proposed to correspond to site I in the hGH structure (5). In both systems this receptor binding site extends from helix A to helix D crossing loop AB. Differences between the two systems lie in the involvement of loop CD in IL-3 and the location of the involved segments in loop AB. Two residues in loop CD (Arg^{94} and Pro^{96}) were found to be important in IL-3, whereas none is in contact with the receptor in GH. The proposed receptor contact site in loop AB of hIL-3 is localized in helix A′ at one end of the loop, whereas it spreads to the mini-helices at both ends of the loop in GH. These differences might reflect a slightly different binding mode or the difference in the size of the two ligand molecules (IL-3 is a short chain cytokine and GH is a long chain cytokine).

Some similarity also exists between the hIL-3 receptor β subunit binding site and GH site II. In both cases, the second site involves helix A and is smaller than the first site. However, helix C of GH is in contact with the receptor, whereas helix C of IL-3 does not appear to be involved in receptor binding. Because no functional epitope has been defined for site II of GH, it is not clear whether the fact that a single residue identified for IL-3 *versus* several residues identified for GH reflects fundamental differences in receptor binding properties for the two proteins or it is only a difference between structural and functional epitopes.

A Structural Model of the IL-3·IL-3 Receptor Complex—The similarity between GH·GHR and IL-3·IL-3R systems permits the modeling of the latter based on the complex structure of the former. As mentioned previously the ligands show little sequence homology but have substantial structural homology (6, 8, 9). The receptors of IL-3 and GH, however, share sequence homology in their extracellular domains consisting of a pattern of conserved Cys residues and the WS*X*WS box near the C terminus (3). The ligand binding domains consist of ~200 amino acid residue cytokine receptor motifs (CRMs) made up of two Ig-like folding domains (3). Although the hGH receptor is a homodimer of identical subunits, the IL-3 receptor is considered a heterodimer composed of distinct α and β chains. Other complications are that the IL-3Rα has an N-terminal domain of ~100 amino acids in addition to the CRM and that the β subunit of IL-3 receptor contains two CRM repeats, while the GH receptor consists of one such motif. For simplicity, we focused on the CRM portion of the α subunit of IL-3 receptor. Due to an earlier report that indicated an interaction between IL-3 and residues 365–368 in the C-terminal motif of the β subunit (29), we considered only the C-terminal (membrane proximal) CRM of the β subunit in our modeling effort.

The IL-3 receptor model is based on the alignment of the human IL-3 receptor sequences with the growth hormone receptor sequence as presented in Fig. 6. It is noted that although receptor sequence alignments in the literature vary somewhat (5, 43), the results presented below are insensitive to small variations. IL-3Rα was constructed on the GHR molecule that contains site I, and the β subunit of IL-3R was built using the GHR molecule in the complex structure that hosts site II (5).

The $hIL\text{-}3_{15–125}$ model could not be superimposed uniquely to GH because IL-3, being a short chain cytokine, is only two-thirds in length compared with the long chain cytokine GH. Thus the docking of $hIL\text{-}3_{15–125}$ to the receptor was guided by the mutagenesis data discussed earlier. A successful receptor-ligand complex model must satisfy the experimental evidence that IL-3Rα contacts Asp^{21} of helix A, Gly^{42}, Glu^{43}, and Gln^{45} of helix A′, and Phe^{113} and Lys^{116} of helix D, and the β_c interacts with Glu^{22} of helix A. Visual inspection of the charge distribution in $hIL\text{-}3_{15–125}$ and its receptor model suggests a docking mode in which two pairs of charge interactions between IL-3 and IL-3Rα can be simultaneously satisfied: Asp^{21} of IL-3 interacts with a cluster of positive charges consists of Arg^{234}, Lys^{235}, and Arg^{277} of the α subunit, which in turn places Glu^{43} of IL-3 in the proximity of Arg^{145} and Arg^{146} of the α subunit. Such a docking leads to a self-consistent IL-3/IL-3Rα interface that will be discussed below. The contact site with the β subunit is rather ambiguous because only a single residue of IL-3 has been identified experimentally. Although residues 365–368 of the β subunit were shown to be crucial for interacting with GM-CSF and IL-5 (29), the moderate decrease in IL-3 binding affinity upon mutations at these sites argues against this region hosting a key interaction with Glu^{22} of IL-3 (18).

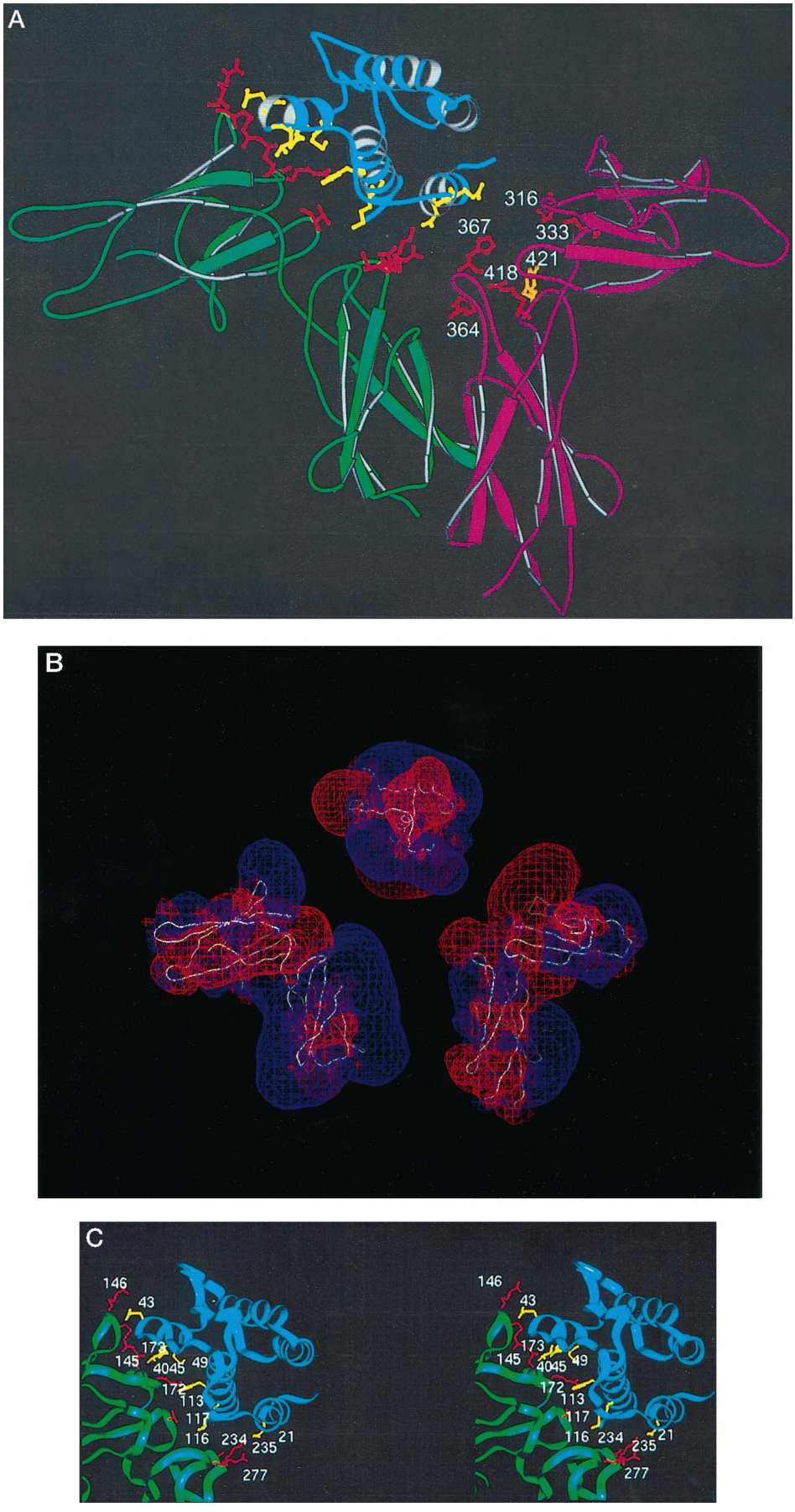
A
316
367
333
421
418
364
B
C
146
43
173
145
4045
49
172
113
117
116
234
235
21
277
146
43
173
145
4045
49
172
113
117
116
234
235
21
277

FIG. 7

Therefore, docking of IL-3 to the β subunit was not attempted, and in the following sections only the putative interface between IL-3 and its receptor α subunit will be discussed in detail.

IL-3/IL-3 Receptor α Subunit Interaction—Upon placing hIL-$3_{15–125}$ into the putative ligand binding pocket by tethering Asp^{21} of IL-3 to Arg^{234}, Lys^{235}, and Arg^{277} of the α subunit and Glu^{43} of IL-3 to Arg^{145} and Arg^{146} of the α subunit (see "Experimental Procedures"), the resulting complex structure is free of severe van der Waals conflicts and consists of an extensive interface between hIL-$3_{15–125}$ and the α subunit (Fig. 7*A*). Furthermore, the electrostatic isopotential surfaces surrounding hIL-$3_{15–125}$ and the receptor α subunit were found to be largely complementary (Fig. 7*B*). The negative potential arising from Glu^{43}, Asp^{46}, and Glu^{50} of IL-3 is complemented by the positive potential generated primarily by Arg^{145} and Arg^{146} of the α subunit. The positive potential near Arg^{108}, Arg^{109}, and Lys^{116} of IL-3 is matched by the negative potential surrounding Asp^{116}, Asp^{118}, and Glu^{276} of the α subunit. A significant amount of surface area of both hIL-$3_{15–125}$ and the α subunit becomes inaccessible to solvent upon formation of the complex (~950 $Å^2$ at the interface). This amount is comparable to that of site I on GH (1230 $Å^2$) (9).

The buried surface area for individual residues in IL-3 and the receptor α subunit at the interface is shown in Fig. 8. Residues in IL-3 that are significantly affected upon binding to the α subunit are (ΔSA >20 $Å^2$): Asp^{21}, Thr^{25}, Leu^{40}, Asn^{41}, Gly^{42}, Glu^{43}, Gln^{45}, Asp^{46}, Met^{49}, Arg^{109}, Phe^{113}, Lys^{116}, Asn^{120}, and Gln^{125}. This list includes most of the important solvent-exposed residues discussed in previous sections. The significantly affected residues in the receptor α subunit are (ΔSA >20 $Å^2$): Val^{117}, Asp^{118}, Arg^{145}, Arg^{146}, Gln^{147}, Arg^{172}, Leu^{173}, Ser^{174}, Ser^{175}, Asn^{233}, Arg^{234}, Lys^{235}, Glu^{276}, Arg^{277}, and Val^{278}.

The development of an IL-3·IL-3R model allowed us to explore the intermolecular interactions on a structural basis. In this model, a number of residues that are hydrophobic or have hydrophobic portion side chains cluster at the center of the interface, as illustrated in Fig. 7*C*. These residues are Leu^{40}, Met^{49}, and Phe^{113} on the ligand side and Val^{117}, Arg^{172}, and Leu^{173} on the receptor α subunit side. Gln^{45} and Lys^{116} of IL-3, which are also indicated in Fig. 7*C*, are located within this cluster. The substitutions (Q45V, K116W, and K116V) to bulky hydrophobic residues at these two sites are thus likely to increase the binding affinity by enhancing the hydrophobic interaction within the cluster. Although Lys^{116} may engage in a salt bridge with Glu^{276} (2.5 Å between the ionizable atoms), the net change in energy when the electrostatic interaction is replaced by hydrophobic interaction can be in favor of the complex formation. Such a net gain in energy can be especially significant considering that a bulky hydrophobic residue at position 116 may extend the hydrophobic cluster to include Phe^{232}, Phe^{236}, Val^{278}, and Tyr^{279} of IL-3Rα (not shown in Fig. 7 for clarity). The elimination of the positive charge at position 116 may fine tune the electrostatic environment near Asp^{21} to facilitate its docking to Arg^{234}, Lys^{235}, and Arg^{277} of the α subunit. Flanking this cluster in the model are two pairs of charge interactions that were used as tether points: Glu^{43} of IL-3 with Arg^{145}/Arg^{146} of the α subunit and Asp^{21} of IL-3 with Arg^{234}/Lys^{235}/Arg^{277} of the α subunit. The model suggests that these electrostatic interactions dock IL-3 into the appropriate position so that the hydrophobic residues can interact efficiently. Such a pattern of a hydrophobic cluster flanked by charged residues resembles the receptor binding site described in GH/GHR system (44). The residues in IL-3Rα that contact the ligand are located in loops AB (Val^{117}), CD (Arg^{145}, Arg^{146}), EF (Arg^{172}, Leu^{173}), B′C′ (Arg^{234}, Lys^{235}), and F′G′ (Arg^{277}), similar to the location of contacts found in the crystal structures of the complex of GH with GHR (9), GH with prolactin receptor (45), and the erythropoietin receptor bound to a peptide agonist (46).

Among the other important residues identified in the previous sections, the mutant G42D can augment the charge interaction between Glu^{43} and Arg^{145}/Arg^{146} by interacting with Arg^{145} (the C_α atom of Gly^{42} is 6.3 Å away from the charge on Arg^{145}), G42A may engage in hydrophobic interaction with Leu^{173} of the α subunit (the C_α atom of Gly^{42} is within 3.5 Å from the methyl groups on Leu^{173}), and D46S can optimize a hydrogen bond with Gln^{147} of the α subunit (the C_γ of Asp^{46} is 6.3 Å away from the C_δ of Gln^{147}). The large surface area buried at the C terminus of hIL-$3_{15–125}$ upon complex formation (see Fig. 8*A*) suggests that the truncation there affects the binding affinity to the receptor α subunit. In the current model, Arg^{94} and Pro^{96} of IL-3 are not in direct contact with the receptor, and their roles remain elusive. It remains possible that Arg^{94}, whose side chain is constrained as indicated by several long range nuclear Overhauser effects to Ile^{47}, compensates the cluster of negative charges at Glu^{43}, Asp^{46}, and Glu^{50} to maintain helix A′ conformation in the absence of the receptor. Alternatively, these two residues may interact with the N-terminal sequence of the α subunit or the membrane distal CRM of the β subunit, neither of which is included in this model.

IL-3/IL-3 Receptor β Subunit Interaction—The interaction between IL-3 and IL-3 receptor β subunit is more difficult to define compared with the α subunit due to the paucity of known contact residues. Experimentally, only Glu^{22} was found to be critical for binding to the β subunit on the ligand side, whereas Tyr^{421} alone was identified as being both necessary and sufficient for high affinity binding and subsequent signaling on the receptor side (47). To date, no experimental data are available that indicate whether these two residues interact with each other or if there is any direct interaction between Tyr^{421} and the ligand. Given these uncertainties, we looked for possible receptor contact sites for Glu^{22} without attempting to dock IL-3 to the β subunit.

Although Glu is capable of forming hydrogen bonds, the severely diminished activity observed for variants E22S, E22H, E22Q, E22H, E22R, and E22Y (19, 20), which should also be able to form hydrogen bonds, suggests that a charge interaction is employed at this contact site. The negative electrostatic potential surrounding Glu^{22} of IL-3 can be compensated by the two patches of positive electrostatic potential located either near Arg^{418}, Arg^{364}, and His^{316} or near His^{367} and Lys^{333} of the β subunit (see Fig. 7, *A* and *B*). These positively charged residues reside in loops EF (His^{316}), GA′ (Lys^{333}), B′C′ (Arg^{364}, His^{367}), and F′G′ (Arg^{418}) of the membrane proximal CRM of the β subunit, similar to the locations of ligand contact sites found in the crystal structures of GHR (9) and the prolactin

Fig. 7. **A complex structure model for hIL-3 and the IL-3 receptor.** *A*, ribbon diagram of the IL-$3_{15–125}$·IL-3R complex structure model based on the crystal structure of the hGH·hGHR complex by Molscript (32). IL-$3_{15–125}$, *cyan*; IL-3 receptor α subunit, *green*; IL-3 receptor β subunit, *magenta*. The residues proposed to be involved in the intermolecular interaction are *highlighted* as ball-and-stick model (see text) (in addition, residue numbers are included for putative interaction sites on β_c). *B*, electrostatic isopotential contour surfaces for the three molecules calculated with GRASP (27). The orientation is approximately the same as in *A* but the distances between the molecules are increased for clarity. The *blue contours* represent the isopotential surface at +0.5 *kT/e* and the *red contours* at −0.5 *kT/e*, where *k* is Boltzmann's constant, *T* is absolute temperature, and *e* is the electron charge. *C*, an enlarged stereo representation of the proposed IL-$3_{15–125}$·IL-3Rα interface (INSIGHT II, Biosym). The residues suggested to be involved in the binding interaction are labeled.

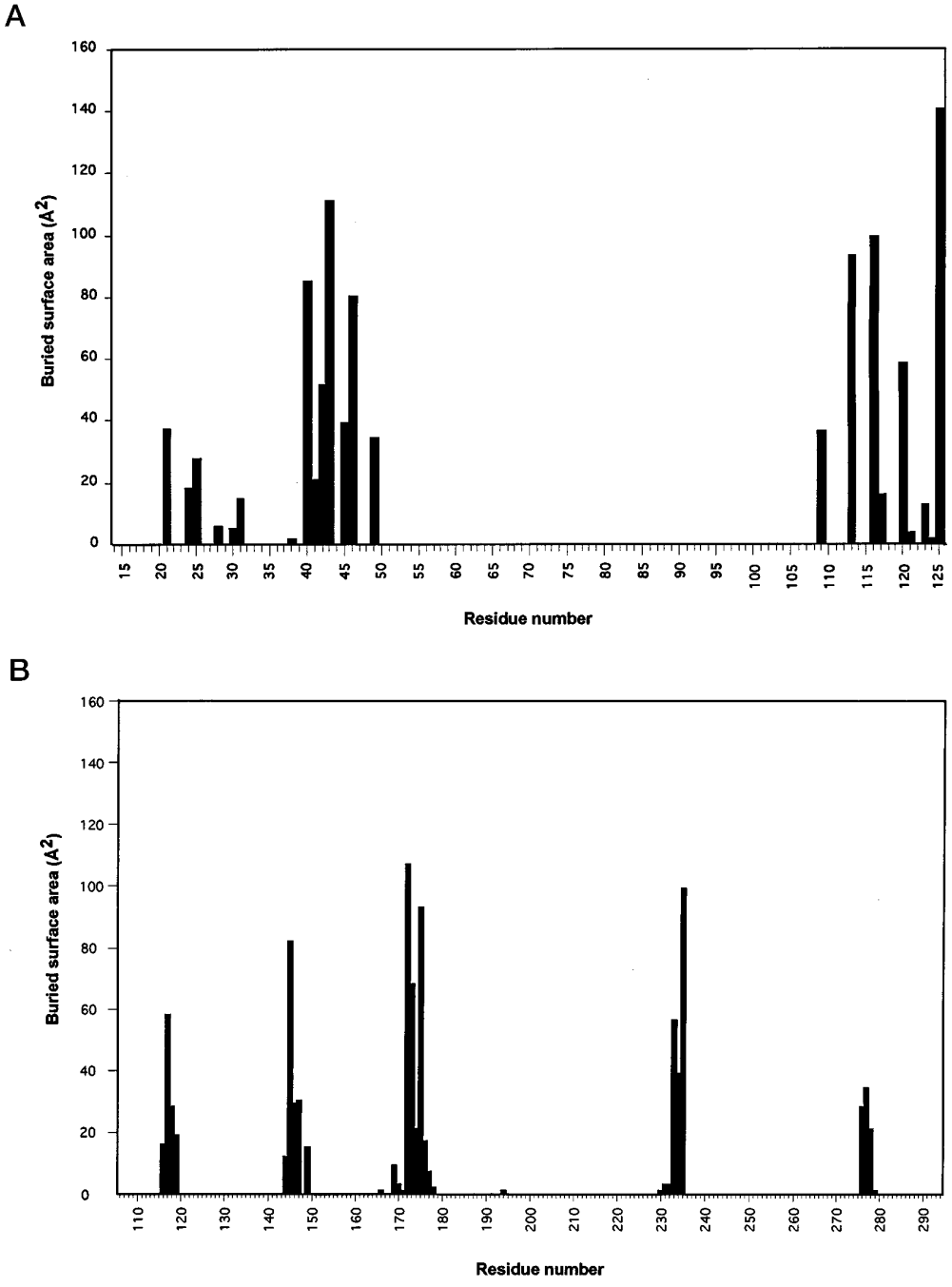

FIG. 8. **hIL-$3_{15–125}$ surface area buried upon complex formation.** Decreases in solvent accessibility for each amino acid residue in the hIL-$3_{15–125}$ model (*A*) and the IL-3Rα model (*B*) upon forming a complex between hIL-$3_{15–125}$ and IL-3Rα. The amount of the buried surface for residues 28–39 of IL-3 may vary significantly because of the flexibility of this loop in the three-dimensional structure.

receptor (45). Inspection of Fig. 7*A* suggests that docking of Glu^{22} to any of these residues could result in a conflict-free interface that would require only a rotation and/or other small adjustments of the β subunit. Mutations at two of these residues, H367A and R418A, have been reported previously (29, 47). Each mutation showed a modest (~4-fold) decrease in the binding affinity of IL-3 to the receptor, suggesting that these residues contribute to the ligand binding but may not be the critical residue(s) of the β subunit that interact with Glu^{22} or that individually they are insufficient to achieve the high affinity binding to the ligand. It will be interesting to mutagenize the remaining three candidates and small clusters of the five residues to test for their involvement individually and collectively.

It is noted that the positive electrostatic potential at Lys^{28} of IL-3 is in the vicinity of a small area of negative electrostatic potential located near Glu^{366} of the β subunit. A distance of 2.5 Å between the side chain nitrogen of Lys^{28} and one of the carboxyl oxygen atoms of Glu^{366} in this model suggests a salt bridge between Lys^{28} of IL-3 and Glu^{366} of the β subunit. Although this interaction may facilitate the proper docking of the ligand, its contribution to the overall binding energy is relatively small considering the 2–4-fold decrease in binding affinity when this potential interaction was disrupted by the E366A mutant of the β subunit (29) or by the K28E mutant of IL-3 (20). The fact that all the solvent-exposed residues of helix A and helix C except Glu^{22} on IL-3 are tolerant to substitution implies that although other residues may also participate in

the interaction with the β subunit, the contribution from each is so modest that they are difficult to identify.

IL-3 Receptor α Subunit/IL-3 Receptor β Subunit Interactions—Although the interface between the two subunits of the receptor was not optimized due to the lack of site-specific experimental data, it is noted in the current model that there is a large positive electrostatic potential surface near the proposed heterodimeric interface on the α subunit, whereas a complementary negative electrostatic potential surface resides on the β subunit. The positive potential surrounds residues Arg^{237}, Arg^{255}, Arg^{257}, and Arg^{277} of the α subunit, and the negative potential arises from Asp^{350}, Glu^{359}, Glu^{427}, Glu^{430}, Asp^{435}, and Glu^{437} of the β subunit. Tyr^{421} of the β subunit, the residue that was found to be crucial for high affinity binding and subsequent signaling (47), is located near this interface and can potentially interact with the α subunit, the ligand, or an auxiliary protein. Recently (48), it was reported that IL-3 induces the formation of both covalent (via disulfide bond formation) and noncovalent heterodimers of the α and β subunits, and disulfide bonds were proposed between IL-3R α and the membrane distal CRM of the β subunit.

Conclusions—The results presented here show that most of the critical residues identified in $hIL\text{-}3_{15–125}$ by mutagenesis are buried within the core of the protein and contribute to the structural integrity, and there is an extensive overlap between these residues and the evolutionary conserved residues. Ten important solvent-exposed residues (Asp^{21}, Gly^{42}, Glu^{43}, Gln^{45}, Asp^{46}, Met^{49}, Arg^{94}, Pro^{96}, Phe^{113}, and Lys^{116}) map to one side of hIL-3 and constitute a putative receptor binding site for the low affinity receptor α subunit, which encompasses regions on helices A and D and adjacent regions in the loops, especially the A′ helix in the first overhand loop. The receptor-ligand complex model suggests that IL-3 binds to the receptor α subunit through hydrophobic interactions anchored by electrostatic interactions. This model leads to hypotheses for critical interactions that can be tested by further experiments incorporating amino acid substitutions into the IL-3 receptor. In the absence of an experimentally derived IL-3·IL-3R complex structure, future mutagenesis data on the receptor will help to refine the receptor-ligand complex model, further our understanding of the IL-3·IL-3R interaction, and lead to the design of improved IL-3 receptor agonists.

Acknowledgments—We thank Chris Bauer, Sarah Braford-Goldberg, Maire Caparon, and Alan Easton for constructing the IL-3 variants; Joe Polazzi for DNA sequencing; Barrett Thiele, Caroline Russell, and Mark Baganoff for purifying many of the single point mutants; Ann Abegg for testing cell proliferation activity of these mutants; John Thomas for help with the receptor binding studies; Russell McKinnie and Cindy Jarvis for circular dichroism measurements; Conrad Halling, David Neidhart, and Neena Summers for helpful discussions on sequence alignments and molecular modeling; and Alan Easton and Peter Olins for helpful discussions. We also acknowledge the support and encouragement of the entire Synthokine Project team.

REFERENCES

1. Metcalf, D. (1991) *Science* **254,** 529–533
2. Schrader, J. W. (1986) *Annu. Rev. Immunol.* **4,** 205–230
3. Bazan, J. F. (1990) *Proc. Natl. Acad. Sci. U. S. A.* **87,** 6934–6938
4. Diederichs, K., Boone, T., and Karplus, P. A. (1991) *Science* **254,** 1779–1782
5. Goodall, G. J., Bagley, C. J., Vadas, M. A., and Lopez, A. F. (1993) *Growth Factors* **8,** 87–97
6. Feng, Y., Klein, B. K., Vu, L., Aykent, S., and McWherter, C. A. (1995) *Biochemisty* **34,** 6540–6551
7. Feng, Y., Klein, B., and McWherter, C. (1996) *J. Mol. Biol.* **259,** 524–541
8. Abdel-Meguid, S. S., Shieh, H.-S., Smith, W. W., Dayringer, H. E., Violand, B. N., and Bentle, L. A. (1987) *Proc. Natl. Acad. Sci. U. S. A.* **84,** 6434–6437
9. deVos, A. M., Ultsch, M., and Kossiakoff, A. (1992) *Science* **255,** 306–312
10. Kitamura, T., Sato, N., Arai, K., and Miyajima, A. (1991) *Cell* **66,** 1165–1174
11. Tavernier, J., Devos, R., Cornelis, S., Tuypens, T., derHeyden, J. V., Fiers, W., and Plaetinck, G. (1991) *Cell* **66,** 1175–1184
12. Kaushansky, K., Shoemaker, S. G., Broudy, V. C., Lin, N., Matous, J. V., Alderman, E. M., Aghajanian, J. D., Szklut, P. J., VanDyke, R. E., Pearce, M. K., and Abrams, J. S. (1992) *J. Clin. Invest.* **90,** 1879–1888
13. Dorssers, L. C. J., Burger, H., Wagemaker, G., and DeKoning, J. P. (1994) *Growth Factors* **11,** 93–104
14. Lokker, N. A., Strittmatter, U., Steiner, C., Fagg, B., Graff, P., Kocher, H. P., and Zenke, G. (1991) *J. Immunol.* **146,** 893–898
15. Lokker, N. A., Zenke, G., Strittmatter, U., Fagg, B., and Movva, N. R. (1991) *EMBO J.* **10,** 2125–2131
16. Dorssers, L. C. J., Mostert, M. C., Burger, H., Janssen, C., Lemson, P. J., van Lambalgen, R., Wagemaker, G., and van Leen, R. W. (1991) *J. Biol. Chem.* **266,** 21310–21317
17. Lopez, A. F., Shannon, M. F., Barry, S., Phillips, J. A., Cambareri, B., Dottore, M., Simmons, P., and Vadas, M. A. (1992) *Proc. Natl. Acad. Sci. U. S. A.* **89,** 11842–11846
18. Barry, S. C., Bagley, C. J., Phillips, J., Dottore, M., Cambareri, B., Moretti, P., D'Andrea, R., Goodall, G. J., Shannon, M. F., Vadas, M. A., and Lopez, A. F. (1994) *J. Biol. Chem.* **269,** 8488–8492
19. Olins, P. O., Bauer, S. C., Braford-Goldberg, S., Sterbenz, K., Polazzi, J. O., Caparon, M. H., Klein, B. K., Easton, A. M., Paik, K., Klover, J. A., Thiele, B. R., and McKearn, J. P. (1995) *J. Biol. Chem.* **270,** 23754–23760
20. Bagley, C. J., Phillips, J., Cambareri, B., Vadas, M. A., and Lopez, A. F. (1996) *J. Biol. Chem.* **271,** 31922–31928
21. Chen, Y. H., Yang, Y. T., and Martinez, H. M. (1972) *Biochemistry* **11,** 4120–4131
22. Thomas, J. W., Baum, C. M., Hood, W. F., Klein, B., Monahan, J. B., Paik, K., Staten, N., Abrams, M., Donnelly, A., and McKearn, J. P. (1995) *Proc. Natl. Acad. Sci. U. S. A.* **92,** 3779–3783
23. Santoli, D., Yang, Y. C., Clark, S. C., Kreider, B. L., Caracciolo, D., and Rovera, G. (1987) *J. Immunol.* **139,** 3348–3354
24. Brunger, A. T. (1988) *J. Mol. Biol.* **203,** 803–816
25. Brunger, A. T. (1992) *A System for X-ray Crystallography and NMR,* X-PLOR Version 3.1, Yale University Press, New Haven, CT
26. Lee, B., and Richards, F. M. (1971) *J. Mol. Biol.* **55,** 379–400
27. Nicholls, A., Sharp, K., and Honig, B. (1991) *Proteins Struct. Funct. Genet.* **11,** 281–296
28. Clark-Lewis, I., Hood, L., and Kent, S. B. H. (1988) *Proc. Natl. Acad. Sci. U. S. A.* **85,** 7897–7901
29. Woodcock, J. M., Zacharakis, B., Plaetinck, G., Bagley, C. J., Qiyu, S., Hercus, T. R., and Travernier, J. (1994) *EMBO J.* **13,** 5176–5185
30. Burger, H., Mostern, M. C., Kok, E. M., Wagemaker, G., and Dorssers, L. C. J. (1994) *Biochim. Biophys. Acta* **217,** 195–198
31. McInnes, C. J., Logan, M., Haig, D., and Wright, F. (1994) *Gene* (*Amst.*) **139,** 289–290
32. Kraulis, P. J. (1991) *J. Appl. Crystallog.* **24,** 946–950
33. Rozarski, D. A., Gronenborn, A. M., Clore, G. M., Bazan, J. F., Bohm, A., Wlodawer, A., Hatada, M., and Karplus, P. A. (1994) *Structure* **2,** 159–173
34. Graber, P., Proudfoot, A. E. I., Talabot, F., Bernard, A., McKinnon, M., Banks, M., Fattah, D., Solari, R., Peitsch, M. C., and Wells, T. N. C. (1995) *J. Biol. Chem.* **270,** 15762–15769
35. Lopez, A. F., Shannon, M. F., Hercus, T., Nicola, N. A., Cambareri, B., Dottore, M., Layton, M. J., Eglinton, L., and Vadas, M. A. (1992) *EMBO J.* **11,** 909–916
36. Hercus, T. R., Cambareri, B., Dottore, M., Woodcock, J., Bagley, C., Vadas, M. A., Shannon, M. F., and Lopez, A. F. (1994) *Blood* **83,** 3500–3508
37. Brown, C. B., Pihl, C. E., and Kaushansky, K. (1994) *Eur. J. Biochem.* **225,** 873–880
38. Shanafelt, A. B., Johnson, K. E., and Kastelein, R. A. (1991) *J. Biol. Chem.* **266,** 13804–13810
39. Kaushansky, K., Shoemaker, S. G., Alfaro, S., and Brown, C. (1989) *Proc. Natl. Acad. Sci. U. S. A.* **86,** 1213–1217
40. Seelig, G. F., Prosise, W. W., and Scheffler, J. E. (1994) *J. Biol. Chem.* **269,** 5548–5553
41. Ultsch, M. H., Somers, W., Kossiakoff, A. A., and deVos, A. M. (1994) *J. Mol. Biol.* **236,** 286–299
42. Cunningham, B. C., and Wells, J. A. (1993) *J. Mol. Biol.* **234,** 554–563
43. Lyne, P. D., Bamborough, P., Duncan, D., and Richards, W. G. (1995) *Protein Sci.* **4,** 2223–2233
44. Clackson, T., and Wells, J. A. (1995) *Science* **267,** 383–386
45. Somers, W., Ultsch, M., DeVos, A. M., and Kossiakoff, A. A. (1994) *Nature* **372,** 478–491
46. Livnah, O., Stura, E. A., Johnson, D. L., Middleton, S. A., Mulcahy, L. S., Wrighton, N. C., Dower, W. J., Jolliffe, L. K., and Wilson, I. A. (1996) *Science* **273,** 464–471
47. Woodcock, J. M., Bagley, C. J., Zacharakis, B., and Lopez, A. F. (1996) *J. Biol. Chem.* **271,** 25999–26006
48. Stomski, F. C., Sun, Q., Bagley, C. J., Woodcock, J., Goodall, G., Andrews, R. K., Berndt, M. C., and Lopez, A. F. (1996) *Mol. Cell. Biol.* **16,** 3035–3046
49. Kabsch, W., and Sander, C. (1983) *Biopolymers* **22,** 2577–2637
50. *UWGCG Software Package* (1991) Version 7.3, Genetics Computer Group, Madison, WI